Yang *et al. Biochar* (2025) 7:5
https://doi.org/10.1007/s42773-024-00395-2

Biochar

ORIGINAL RESEARCH Open Access

Role of sludge biochar immobilized multifunctional microbiome in phytoremediation of lead-zinc composite pollution

Zihao Yang[1], Lijuan Jiang[1], Xuejun Li[3], Qiaoling Ji[1], Mengyuan Wang[1], Yi Zhang[3], Yuanlin Cheng[3], Xuan Zhang[2*], Hui Li[2*] and Chongling Feng[1*]

Abstract

Sludge biochar, as a soil amendment, has demonstrated its capacity to remediate heavy metal-contaminated soil. It is frequently utilized to facilitate phytoremediation or as a microbial carrier in remediation strategies, aiming to enhance overall remediation efficiency. Nonetheless, there exists a knowledge gap regarding the influence of biochar on the migration and accumulation of Pb and Zn within soil-microbe-plant systems, as well as its effects on plant growth conditions and microbial community composition. This study constructed a multifunctional microbiome and evaluated the role of microbiome and biochar in phytoremediation under Pb and Zn stress. Biochar immobilized microbiome (MB) significantly enhanced phytoremediation and showed synergistic effects by improving root phenotypes up to 2.4 times compared to the untreated group (CK). Meanwhile, the MB increased Pb root absorption by 56.9% and Zn above-ground transfer by 30%, and reduced the acid-extractable content of Pb and Zn under high concentrations. In addition, microbial community composition and diversity analyses showed that the bacterial and fungal communities of MB were more stable while multifunctional microbiome reshaped microbial community with boosted abundance of plant growth promoting microorganisms, and fungi of saprotroph and symbiotroph nutritional categories. This study provided a novel phytoremediation approach of castor with the combination of multifunctional microbiome and biochar.

Highlights

- Castor effectively transfers Zn to aboveground parts (TFmax = 2.89).
- Natural slag was detrimental to root growth, with 60.6% decrease in phenotypes.
- MB synergistically enhanced root length, surface area, tip, and volume to 2.4 times.
- MB increased Pb root absorption by 56.9% and Zn above-ground transfer by 30%.
- Multifunctional microbiome boosted the abundance of PGPRs.

*Correspondence:
Xuan Zhang
zhangxuansherry@163.com
Hui Li
lihuiluoyang@163.com
Chongling Feng
ddukepet@163.com
Full list of author information is available at the end of the article

Keywords Biochar, Bioremediation, Pb, Zn, *Ricinus communist* L.

Graphical Abstract

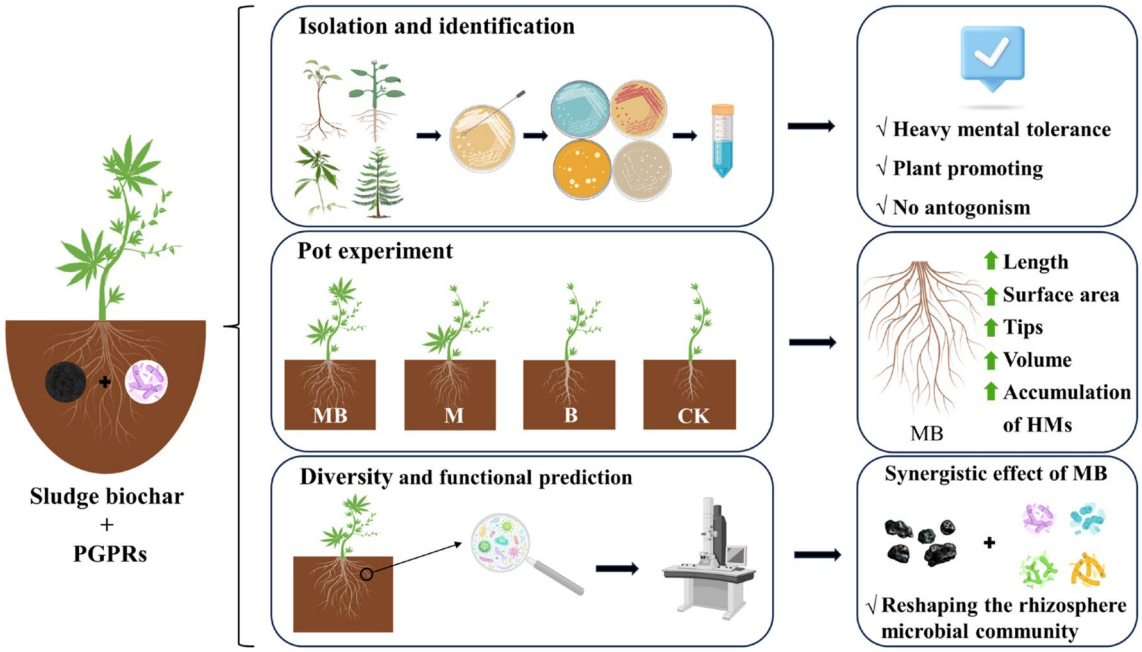

1 Introduction

Heavy metal (HM) pollution, originating mainly from metal smelting and dumping, presents a significant threat to global environmental and human health (Liu et al. 2018; Xu et al. 2021). Soil remediation is imperative due to HM's high carcinogenic, genotoxic, and neurotoxic properties (Luo et al. 2023). HMs such as lead (Pb) and zinc (Zn) are of concerns as they are top priorities on the United States Environmental Protection Agency (US EPA) control list, observed or assumed to be highly harmful to humans (Peng et al. 2022). Pb and Zn are often found as co-pollutants (Abedi et al. 2022), left in topsoil due to industrial activities, ultimately threatening human health through the food chain (Li et al. 2015). Blind mining, tailings, and indiscriminate wastewater discharge after ore smelting are the leading causes of Pb and Zn contamination in mine soils (Cao et al. 2022a). According to statistics, Pb/Zn mining and smelting activities release approximately 357 to 857×10^6 kg of Pb and 462 to 1380×10^6 kg of Zn into the environment every year (Zhang et al. 2012). Pb is considered a potential carcinogen and has been linked to the etiology of many diseases, especially cardiovascular, liver, kidney, bladder, nervous system, blood, and bone disorders (Cai et al. 2019). Zn is a nutrient available to the human body. It is involved in development and metabolic processes in the human body, but excessive metal intake can cause fatigue and dizziness (Anwar et al. 2016). These metals can cause damage to the human reproductive and central nervous systems as they can accumulate in the organisms (Xia et al. 2019).

As a form of bioremediation, phytoremediation can utilize the absorption and accumulation functions of plants and associated soil microorganisms to reduce the concentration or toxic effects of pollutants in the environment (Ali et al. 2013). Contaminated soil produced by smelting and dumping has characteristics such as high pH, high salinity, low water retention capacity, high HM concentrations, and deficiencies in soil organic matter and fertility (Wang et al. 2017). Therefore, it is necessary to select reliable in situ phytoremediation plants. *Ricinus communist* L. (castor) is a typical energy plant that has been considered for remediation of contaminated soil while providing economic value due to its bioenergy production capacity and tolerance to biotic and abiotic stresses (Bauddh et al. 2015; Zhang et al. 2016). Previous studies have demonstrated that castor exhibits high tolerance and accumulation capacity to high concentrations of

HMs such as Cd, Zn, Pb, Cu, and Cr (He et al. 2020). In this study, castor was selected as the remediation plant of Pb–Zn composite contaminated soil.

In recent years, there has been increasing evidence that plant rhizosphere-associated microorganisms can promote plant growth in contaminated soils and improve the phytoremediation efficiency of polymetallic-contaminated soils (Yao et al. 2023). Microorganisms that can colonize and proliferate within the rhizosphere of plants and have the ability to promote plant growth are called plant growth-promoting rhizobacteria (PGPR) (Beneduzi et al. 2012). PGPR enhance phytoremediation in several ways, such as providing nutrients to plants, releasing growth regulators, inducing systemic resistance, and altering the bioavailability of HMs in the soil (Chen et al. 2022; Fan et al. 2024; Lai-Guo and Yong 2004). Although PGPR can adapt to various adverse environments, bioremediation efficiency is limited by microbial biomass and nutrients (Zhang et al. 2021). Given the potential additive or synergistic effects of PGPR in pollutant degradation and remediation, the outcomes of phytoremediation can be attributed to the total microbiome and its dynamic interplay with the host plant rather than to a single microorganism (Hibbing et al. 2010; Thijs et al. 2017). Reasonable selection of microbiome will effectively bring out the characteristics of each microorganism (Simmer and Schnoor 2022), thus to combine composite PGPRs into a multifunctional microbiome which could be a reliable option for remediating complex contaminated environments (Bertrand et al. 2014).

Except for composed microbiome, biochar was chosen as a soil amendment in many cases. Regarded as a carbon-rich material produced by the combustion of organic raw materials under pure heat and limited oxygen, biochar is commonly used to improve soil fertility and carbon sequestration (Joseph et al. 2021; Li et al. 2023b). Biochar remains stable and unaffected by biological and chemical degradation when applied to the soil, promotes plant growth, enhances microbial activity, and is believed to improve the phytoremediation efficiency of hyperaccumulators (Ghosh and Maiti 2021; Kiran and Prasad 2019). Compared to other commonly used biomass-derived biochar, sludge biochar is attractive due to its phosphorus and silica rich properties (Chen et al. 2019). Sludge, produced during wastewater treatment, is a solid waste that requires treatment and disposal; however, it is a promising feedstock for biochar production, and the resulting biochar is known as sludge biochar. (Wang and Wang 2019). It has been reported that sludge biochar can stabilize HMs directly through chemical action or phytostabilization, leading to improved tailings' pH, TC, and TN contents (Li et al. 2023a). Previous studies have found that sludge biochar is effective in improving soil quality and nutrients and can increase crop productivity (Chen et al. 2020; Figueiredo et al. 2019; Singh et al. 2020). Despite the significant role of sludge biochar in improving soil fertility and nitrogen fixation, there are few studies on the enhancement of HM accumulation in plants by sludge biochar and the combined application of sludge biochar with multifunctional microbiome (Kiran and Prasad 2019; Zhang et al. 2021).

To expand the understanding of the advantages of multifunctional microbiomes and their interactions with biochar in contaminated soils, this study isolated and screened rhizosphere microorganisms with high HM tolerance and PGPR potential from the rhizosphere soil of pioneer plants in HM-polluted tailings to construct a efficient multifunctional microbiome. Additionally, the study explored the synergistic effects of the multifunctional microbiome and sludge biochar on phytoremediation under various Pb–Zn stress conditions, particularly under the extreme values of natural Pb–Zn pollution represented by slag. This research provides novel insights into the mechanisms governing Pb–Zn transport, transformation, and bioavailability, emphasizing the significant impact of integrating sludge biochar and microbiomes in the phytoremediation of Pb–Zn contaminated soils.

2 Materials and methods

2.1 Sampling, strain isolation, and screening

The soil samples for strain isolation in this study were taken from the rhizosphere soils of phytoremediation plants (*Paulownia tormentosa* Thunb. (paulownia), *Koelreuteria paniculata* Laxm. (goldenrain), *Cinnamomum camphora* Linn. (camphor), and *Boehmeria nivea* L. (ramie) used in the Pb–Zn mine tailing, located at the southeast of Chenzhou, Hunan, China (113°09′00″ E, 25°44′46″ N).

The soil tightly bound to the plant roots is collected as rhizosphere soil (Supplementary S1). Fresh rhizosphere soils of the four phytoremediation plants were mixed with sterile water and diluted into 10^{-4} soil solutions. Aliquots (0.1 mL) were plated onto five isolation media (WA, TWYE, MS, IPS4 and HV) (Table S1), incubated at 28 °C for 3 days. Colonies showing different characteristics were isolated and subcultured on PDA medium and LB medium, respectively, depending on their fungal or bacterial nature.

2.2 HM tolerance test

Microorganisms from rhizospheres were tested for MICs of Pb and Zn according to standard protocols (Wiegand et al. 2008). Strains that tolerated both Pb and Zn concentrations exceeding 600 mg L^{-1} were selected for further study.

2.3 DNA extraction and identification of bacteria and fungi

The 16S and ITS rRNA methods for identification of bacteria and fungi were carried out separately. Bacterial samples underwent denaturation and PCR amplification with primers 27F (5′-AGAGTTTGATCCTGGCTCAG-3′), 1492R (5′-GGTTACCTTACGACTT-3′), while fungal samples used primers ITS1 (5′-TCCGTAGGTGAACCTGCGG-3′), ITS4 (5′-TCCTCCGCTTATTGATATGC-3′). Genomic DNA underwent PCR amplification with the respective primers, followed by bidirectional sequencing and BLAST analysis on the NCBI database for identification (Boratyn et al. 2013).

2.4 Characterization of strains' plant growth promoting (PGP) traits

2.4.1 Phosphate solubility

The phosphorus solubilizing ability of the strains was determined by inoculating 20 µL of the bacterial suspension in the center of the NBRIP medium test medium, incubating at 28 °C within 6 days, and observing whether a hyaline ring formed around the strain (Nautiyal 1999).

2.4.2 Nitrogen fixation capacity

The nitrogen fixation capacity of the strains was determined by inoculating 20 µL of bacterial suspension in the center of Ashby's medium, incubating at 28 °C for 72 h, and observing the growth size and color of the strains (Kizilkaya 2009).

2.4.3 IAA production capacity

The determination of IAA production is based on colorimetric assay (Fan et al. 2018). Strains were inoculated on LB agar medium with 0.5 mg L^{-1} tryptophan and incubated at 28 °C with agitation for 2 days (bacteria) or 7 d (fungi). After centrifugation, 1 mL of supernatant was mixed with Sackowski's reagent. A red color indicates IAA production.

2.4.4 ACC deaminase activity

A 20 µL spore solution (10^8 CFU mL^{-1}) of fungus was inoculated into DF medium and incubated at 28 °C for 7 days (Penrose and Glick 2003). ACC deaminase-positive fungi showed significant growth in DF medium. Bacterial solutions were added to DF and DFa media at a 1:100 ratio and incubated at 28 °C. OD_{600} values were measured at 12, 24, and 48 h to assess bacterial growth, with DF medium as the control.

2.5 HM removal rates of strains

Bacteria ($OD_{600} \approx 1.0$) and fungi (10^{12} CFU mL^{-1}) were inoculated into LB broth and PDB medium containing 5 mL 4000 mg L^{-1} Pb^{2+} and Zn^{2+} , respectively at 28 °C. Sampling was performed every 12 h. After the sample was filtered through a 0.44 um cellulose acetate membrane, flame atomic absorption spectrophotometry (FAAS) was used to determine the Pb and Zn concentrations of the filtrate.

To calculate the removal efficiency of HMs from the soil, the following equation was used (Wang et al. 2019):

$$q = \frac{C_0 - C}{C} \times 100\%$$

where C_0 and C represent the initial and equilibrium Pb/Zn concentration in the solution, respectively.

2.6 Strain antagonism test and composite colonies construction

2.6.1 Strain antagonism experiments

Microbial antagonism among 18 screened resistant strains was evaluated on PDA agar medium (Figure S1). Inhibition zones were measured to determine antagonistic activity. Distances greater than 3 cm indicated strong antagonism, while those between 1.5 and 2.5 cm were considered moderate, and distances less than 1.5 cm indicated no antagonism (Arasu et al. 2013).

2.6.2 Multifunctional microbiome preparation

A total of 5 strains of microorganisms were selected as the foundational strains for constructing a multifunctional microbiome. The bacterial cultures were prepared to reach an OD_{600} of 1, while the fungal cultures were prepared to contain 10^{12} CFU mL^{-1} of spores. The resuspensions of different strains were mixed in equal volumes to prepare a multifunctional microbiome.

2.7 Biochar used in the experiment

The sludge biochar applied in the experiment was prepared by pyrolysis of sludge using a stationary pyrolysis bed at 700 °C. The properties of the biochar are shown in Table S3.

2.8 Biochar immobilized microbiome

The biochar passed through a 60-mesh sieve and the microbiome suspension was mixed at a ratio of 1:10 (m/v), cultured at 30 °C for 24 h, filtered, fully washed, and vacuum freeze-dried for 24 h to obtain biochar-immobilized microbiome (Ji et al. 2022).

2.9 Pot experiment

Pots with 18 cm diameter and 12 cm height containing 1.5 kg of soil matrix were used. Quartz sand (1:1, v/v) to increase permeability was added. Each pot was transplanted with three sterile castor seedlings. The treatments for the pot experiment were as follows: single

Pb^{2+} stress (concentration mg kg^{-1}): CK (0), PCK1 (100), PCK2 (300), PCK3 (700); single Zn^{2+} stress (concentration mg kg^{-1}): CK (0), ZCK1 (250), ZCK2 (400), ZCK3 (800); Pb–Zn composite contaminated soil (mg kg^{-1}): TCK1 ($200Pb^{2+}$, $400Zn^{2+}$), TCK2 ($400Pb^{2+}$, $600Zn^{2+}$), TCKD ($1090Pb^{2+}$, $2268Zn^{2+}$). D stands for natural slag (Table S4). Four different treatments were designed under each concentration: CK is the blank control (plants only); M stands for the addition of multifunctional microbiome (4 mL inoculum per 20 d); B represents the treatment of adding 5% (w/w) biochar; MB is the treatment of adding 5% biochar-immobilized microbiome. Each treatment had 6 replications. Plants were grown under natural light conditions with a soil moisture content maintained at 60%. All plants were harvested after 60 d.

2.10 Plant analysis

2.10.1 Plant biomass determination

Whole plants were uprooted, washed, and placed in sealed bags for analysis. Root length, plant height, and biomass were measured with precision stainless steel tape measures. Fresh and dry weights were determined after rinsing and desiccation (Figure S2, Table S6).

2.10.2 Pb and Zn uptake, translocation and accumulation

Prior to plant Pb/Zn determination, plants were washed, dried, and powdered. A 0.25 g sample was digested with concentrated nitric acid and perchloric acid (HNO_3–$HClO_4$) until colorless (Afonso et al. 2019). Pb and Zn contents were analyzed by flame atomic absorption spectrophotometry.

Transfer factor (TF), the ratio of HM concentration in the stem to the root of the plant was calculated using the following equation (Suo et al. 2021):

$$TF = HM_{shoot}/HM_{root}.$$

where HM_{shoot} and HM_{root} are HM concentrations in the aboveground and belowground, respectively.

2.11 Acid extractable state of Zn and Pb in rhizosphere soil

The determination of acid-extractable Pb and Zn in soil was carried out by acetic acid extraction method. Soil samples (0.5 g) were added to 0.11 M acetic acid at a solid-to-water ratio of 1:40 (w/v) in centrifuge tubes. The suspensions were shaken at 180 rpm for 16 h at 25 °C, then centrifuged and filtered through a 0.45-μm filter membrane. Pb and Zn concentrations were measured by inductively coupled plasma optical emission spectrometer (ICPOES, PerkinElmer, Optima 5300 DV, USA).

2.12 Statistical analysis

The data were presented as means ± standard deviation (SD) from a minimum of 3 replicates. Data were processed using Excel and Minitab 9.0 and presented as mean ± standard deviation (SD) of the three datasets. Differences between treatments were assessed using one-way analysis of variance (ANOVA) followed by Tukey's test. Significance was denoted by different lowercase letters above the bar graphs at $p < 0.05$. Graphs were generated using Origin 9.0. Functional composition of bacterial communities was predicted using PICRUSt2, while FUNGild was utilized to predict functional guilds of fungal communities.

3 Results and discussion

3.1 Isolation, identification of strains and microbiome construction

3.1.1 Characterization of the MB

Figure 1 presents SEM images of sludge biochar and MB. The porous structure on the surface of sludge biochar provides a good habitat for microbial colonization, protecting microorganisms from the direct toxicity of Pb and Zn. Furthermore, SEM images of MB recovered under high stress concentrations showed noticeable fungal hyphae and bacterial cells, indicating the effective immobilization of the multifunctional microbial consortium.

FTIR spectra (Fig. 2) provided information on the functional groups present on the surface of biochar and MB under different metal stress conditions. Due to the high content of aromatic structures and phenolic compounds in sludge biochar, the peak at 992 cm^{-1} may be attributed to the C–O bond and the stretching vibration of C–C in aromatic rings (Singh et al. 2020). The peak at 1620 cm^{-1} is due to the C=O stretching vibration, indicating the presence of carbonyl groups (Zhang et al. 2020b). The peak at 777 cm^{-1} is assigned to aromatic C–H (Tian et al. 2021). After HM stress treatment, the peaks at 1620, 992, and 777 cm^{-1} in MB all weakened, suggesting that Pb^{2+} and Zn^{2+} interacted with C=O, C–C, and C–H in the aromatic rings, indicating the physical adsorption of Pb^{2+} and Zn^{2+} by MB (Chen et al. 2023; Zhang et al. 2019).

3.1.2 Screening of Pb and Zn tolerant strains

There were 78 strains isolated from the rhizosphere soil in the mining area, including 38 fungi and 40 bacteria (Table S2). Fifteen strains with high tolerance were identified (Table 1). The maximum MIC values of the strain are 2000 mg L^{-1} for Pb and 1600 mg L^{-1} for Zn. Four strains were found to have the highest HM removal capacities, i.e. *Klebsiella pneumoniae* P1, *Klebsiella pneumoniae* P2, and *Bacillus sp.* P3, with 75.33%, 66.00%, and 64.67% removal rates of Pb, and 65.67%, 60.33%, and 71.67% of Zn, respectively. Fungi strain *Aspergillus niger* L4 removed 57.33% of Pb and 77.33% of Zn. Strains were screened for Pb and Zn tolerance, with those tolerating

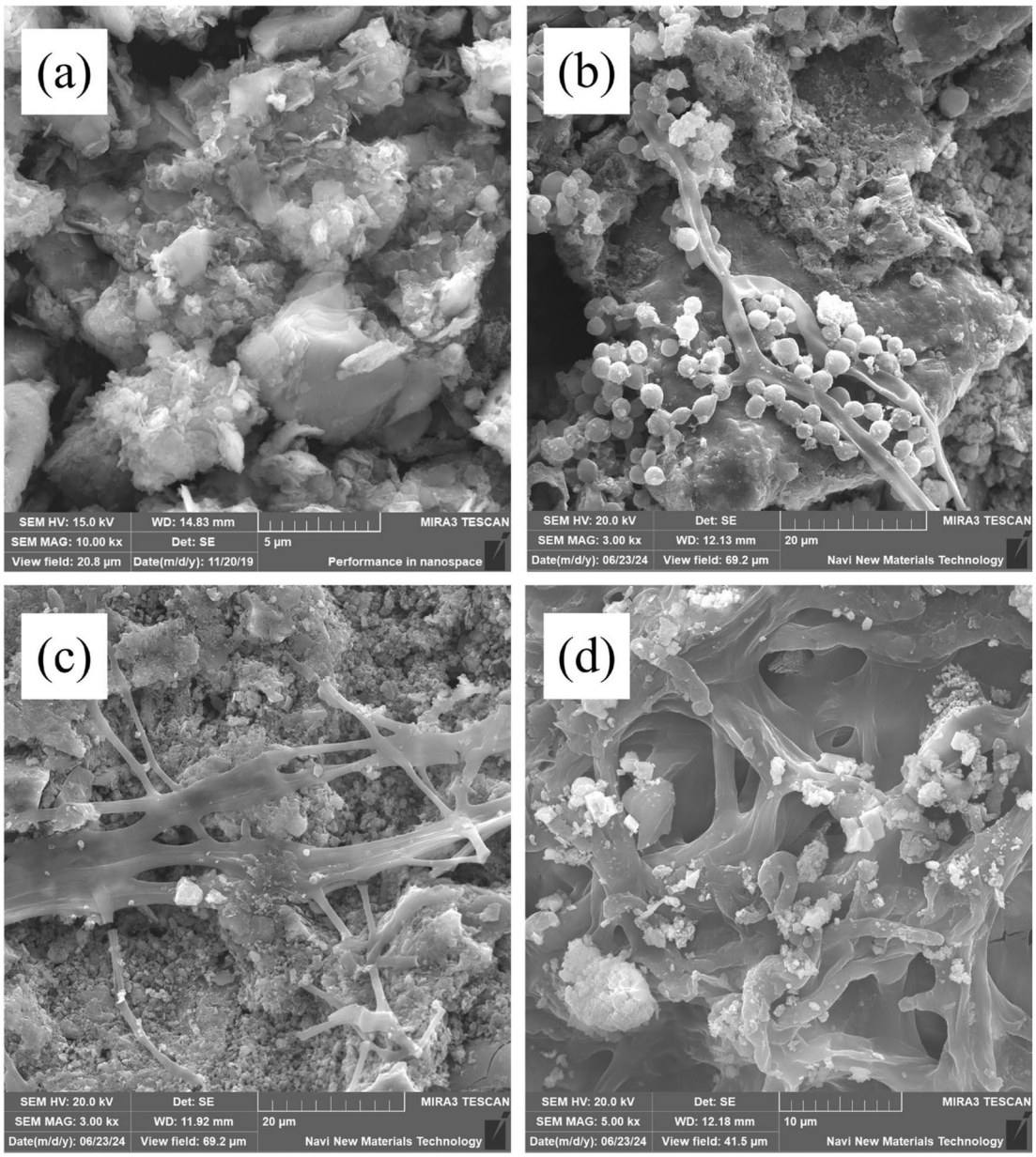

Fig. 1 SEM images of **a** sludge biochar, **b** MB under Pb (700 mg kg^{-1}) stress, **c** MB under Zn (800 mg kg^{-1}) stress, **d** MB under slag stress

higher than 600 mg L^{-1} values were selected for PGP traits evaluation.

3.1.3 Plant-promoting characterization of tolerant strains

The expression of PGP traits will provide further basis for the construction of multifunctional microbiome. As shown in Table 1, *Klebsiella pneumoniae* P1, *Bacillus* sp. P3, *Aspergillus niger* L4, *Purpureocillium lilacinum* L9, *Purpureocillium lilacinum* L10, and *Penicillium* sp. nov. L12 had good phosphorus solubilization, nitrogen fixation, IAA production, and ACC production performance. To enhance the diversity of strains, HM-resistant strains N16 (*Methylobacterium*), N5 (*Talaromyces marneffei*), and N8 (*Trichoderma asperellum*) with robust growth-promoting properties were introduced for subsequent experiments. The effectiveness of phosphorus in soil is usually low, and those strains with phosphorus solubilization capacity can increase the bioavailability of phosphorus for plant uptake (Deng et al. 2024; Etesami et al. 2021). Nitrogen is the most limiting element in ecosystems and crop production, and more than 60% of fixed nitrogen comes from biological nitrogen fixation. Thus,

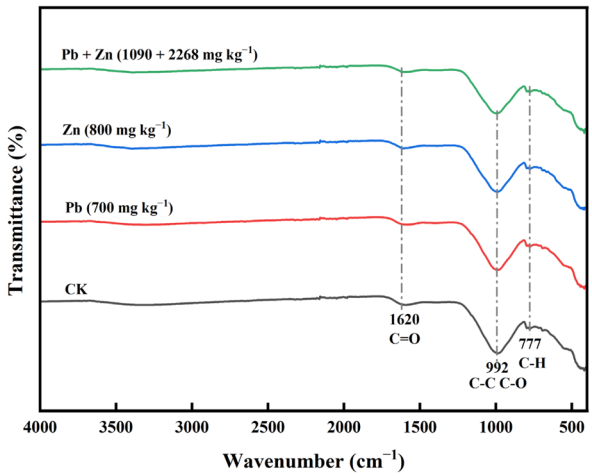

Fig. 2 FTIR spectra of MB under different stresses

microorganisms' nitrogen fixation capacity is significant for plant growth in phytoremediation (Soumare et al. 2020). Microorganisms with IAA-producing ability have been found to improve plant growth by promoting root and shoot development (Lobo et al. 2022; Shahzad et al. 2017). Strains P3 and L4 were observed to possess higher levels of IAA production, phosphorus solubilization, and nitrogen fixation abilities, and will be considered for subsequent potting experiments. Another critical mechanism by which plant growth-promoting fungi promote the growth of plant is the reduction of ethylene levels in plants via ACC deaminase (Glick et al. 2007). Therefore, strains N16, N5, and N8 with higher ACC deaminase activity may have the potential to promote plant growth. These strains will be considered as foundational components for constructing multifunctional microbiome. A total of 18 strains were subjected to plate confrontation experiments (Table 1, Fig. S1), since to construct microbiome, individual strains should share common substrate, and their spatial proximity to each other is preferably synergistic interactions (Mille-Lindblom and Tranvik 2003). The results showed that except for the antagonistic effect observed among L12, M14 and P1, there was no significant mutual inhibitory effects observed between the remaining strains. We hypothesized that competition for organic energy and the production by bacteria of fungal-inhibiting volatiles led to antagonism between bacteria and fungi (Hannula et al. 2017; Li et al. 2020). However, certain interactions between them may be mutually beneficial, such as when bacteria stimulate fungal growth and enhance fungal diversity (Baudy et al. 2021). Based on their growth-promoting performance, HM removal rates, and antagonistic effects, strains P3, L4, N16, N5, and N8 were selected as foundational components for constructing multifunctional microbiome. These strains were subsequently introduced into soil for potting experiments.

3.2 Enhancement of castor plant growth and resistance to Pb and Zn

3.2.1 Effects on root development of castor

Figure 3 depicts the variations in root length, surface area, tip number, and volume of castor plants across different treatment groups. Each root index was further subdivided into four treatment groups to illustrate changes within each group as HM concentrations varied. Notably, MB treatment consistently enhanced root indexes compared to other treatments under varying HM stress. The observed patterns highlight the synergistic effects of biochar and multifunctional microbiome in promoting plant growth. The introduction of biochar (Table S3) improves soil physicochemical properties and promotes plant growth (Wang et al. 2020), while the multifunctional microbiome with good PGP performance (Table 1) further promotes plant root cell division and nutrient utilization (Goswami et al. 2016; Vacheron et al. 2013).

Under Pb and Zn stress, a trend of "low promotion and high inhibition" was noted. Specifically, under single Pb stress (Fig. 3a), optimal root development occurred at a Pb concentration of 300 mg kg^{-1}, beyond which root parameters were suppressed. Similarly, under Zn stress (Fig. 3b), optimal root development was observed at 400 mg kg^{-1} Zn, with severe inhibition at 800 mg kg^{-1}. Subsequently, we examined plant root growth under combined Pb–Zn stress (Fig. 3c). The TCK1 treatment group, exposed to a compound pollution treatment, exhibited the most favorable root development, followed by TCK2. Conversely, as Pb–Zn concentration increased, the TCKD group experienced inhibited root development indices, with a decrease averaging 60.64%, 49.95%, 39.69%, and 53.09% across each root index compared to the control group. The combined stress induced by slag, characterized by higher concentrations of Pb and Zn, has obvious adverse effects on plant root phenotypes. This phenomenon is likely related to the biotoxicity of Pb and Zn, which inhibits cell division in the root tip at high concentrations (Fahr et al. 2013; Kaur and Garg 2021).

In this study, we observed a significant plant root growth and development promotion by adding microbiome with biochar at specific stress concentrations. Roots are one of the most crucial nutrient organs of plants and a significant location for productive symbiosis between microorganisms and plants (Ghahremani and MacLean 2021). In response to environmental stresses, rhizosphere microorganisms often establish beneficial interactions with plants and help regulate root meristem plasticity (Li et al. 2024). It explains the

Table 1 Determination of minimum inhibitory concentration (MIC) of HMs and Pb and Zn removal ability of 18 highly tolerant strains

	Strain	IAA production	Phosphate solubilization	Nitrogen fixation	ACC deaminase activity	Antagonism	MIC (mg L^{-1})		Removal rate (%)	
							Pb^{2+}	Zn^{2+}	Pb	Zn
Bacteria	*Klebsiella pneumoniae* P1	+ +	+	+ + + +	−	−	1000	800	75.33	65.67
	Klebsiella pneumoniae P2	+	+	+	−	−	1000	600	66.00	59.33
	Bacillus sp. P3	+ + +	+ +	+ + + +	−	−	1200	1000	64.67	71.67
	Ochrobactrum sp. nov. P6	+ +	+ +	+	−	−	1200	1000	37.00	53.67
	Ochrobactrum L7	+ +	−	+ + +	−	−	1400	1000	59.33	51.67
	Bacillus altitudinis L8	−	−	+ + +	−	−	1400	1000	55.33	57.67
	Methylobacterium N16	+ + + +	+	+ + + +	+ +	−	1000	600	66.00	59.33
Fungi	*Aspergillus niger* L4	+ + + +	+ + +	+ + + +	−	−	2000	1200	57.33	77.33
	Aspergillus M5	−	−	+	+	−	1000	1600	50.67	57.33
	Purpureocillium lilacinum L9	+ +	−	+ + + +	−	−	2000	1600	53.67	67.67
	Purpureocillium lilacinum L10	+ +	+	+ + + +	−	−	2000	1600	47.67	64.33
	Aspergillus niger L11	+ + +	+	+	−	−	1000	800	57.67	64.33
	Penicillium sp. nov. L12	+ +	+	+ + +	−	+(P1)	1600	1200	42.00	56.67
	Penicillium sp. nov. L13	−	+	+	−	−	1400	1000	45.67	57.67
	Penicillium sp. nov. M14	+	−	+ +	−	+(P1)	1000	800	54.33	66.67
	Penicillium sp. nov. M15	−	−	+	−	−	1000	800	54.33	62.00
	Talaromyces marneffei N5	+ +	+	+ + + +	+	−	1000	600	59.33	64.33
	Trichoderma asperellum N8	+ +	+	+ + + +	+	−	1000	1800	65.67	64.33

Identification of these strains along with their growth promotion and antagonistic properties is also presented. "+" denotes the strength of growth promotion and antagonism; "−" denotes absence of growth promotion or antagonism

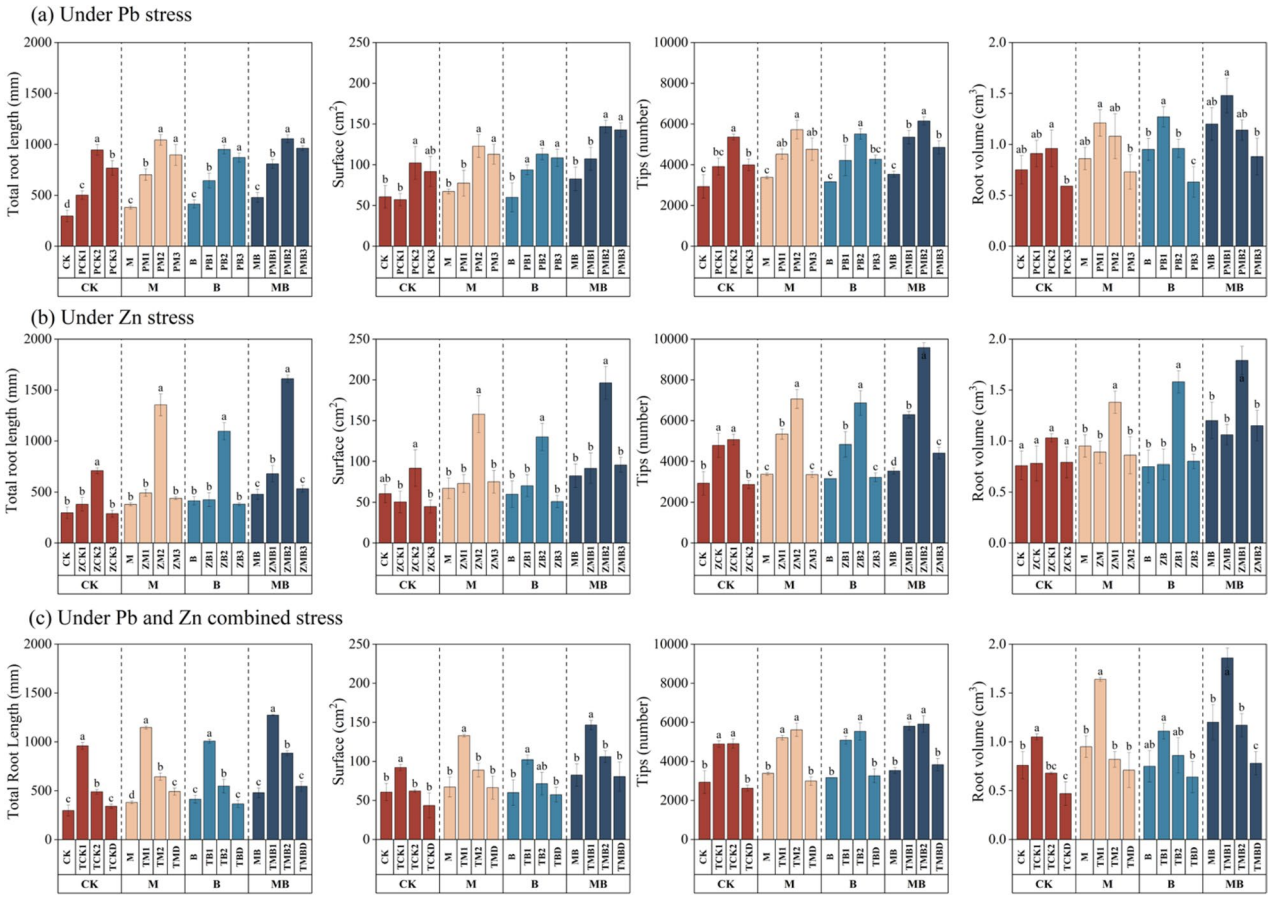

Fig. 3 The root length, root surface area, number of root tips, and root volume of castor under different treatments from left to right. **a** and **b** represent the single stress of Pb and Zn, respectively, and **c** represents the combined stress of Pb and Zn, and each root index was divided into four treatment groups in order to show the trend of changes within each treatment group when HM concentrations were varied

inclusion of a complex microbiome assisted by biochar, which showed varying degrees of response in root length, root surface area, root tip number, and root volume compared to the control. These rhizosphere microorganisms are also known as plant growth-promoting rhizobacteria (PGPR). PGRP promote plant growth through nitrogen fixation and competition with pathogenic bacteria (Adesemoye et al. 2009; Lugtenberg and Kamilova 2009). In addition, various phytohormones produced by PGRP have been widely reported as microbial chemicals that regulate plant root development (Khan et al. 2020). IAA is the most typical phytohormone produced during this growth-promoting process, and the production of IAA has been implicated as one of the significant factors in the microbial induction of root development and growth promotion (Aloni et al. 2006; Spaepen et al. 2007; van Loon 2007). Therefore, we inferred that the process of increased root indexes in castor is the result of the additional nutrition provided by sludge biochar and the dominance of microbiome in the performance of nitrogen fixation, IAA production, and other pro-growth functions.

3.2.2 Impact on the accumulation of Pb and Zn in castor

Under singular stress conditions (Fig. 4a), plants exhibited markedly distinct uptake patterns for Pb and Zn. Specifically, Pb tends to be sequestered in the belowground parts of plants, with a positive correlation observed between stress concentration and root-fixed concentration. Notably, compared to CK (195.49 mg kg^{-1}), the highest root fixation level (398.52 mg kg^{-1}) was recorded in the MB treatment under a Pb stress concentration of 700 mg kg^{-1}. Conversely, Zn demonstrates a preference for aboveground translocation, with the highest aboveground accumulation level (240.20 mg kg^{-1}) attained under the MB treatment at a stress concentration of 800 mg kg^{-1}.

Furthermore, we evaluated the TF index (Table S5), which reflects the root crown's capacity for HM

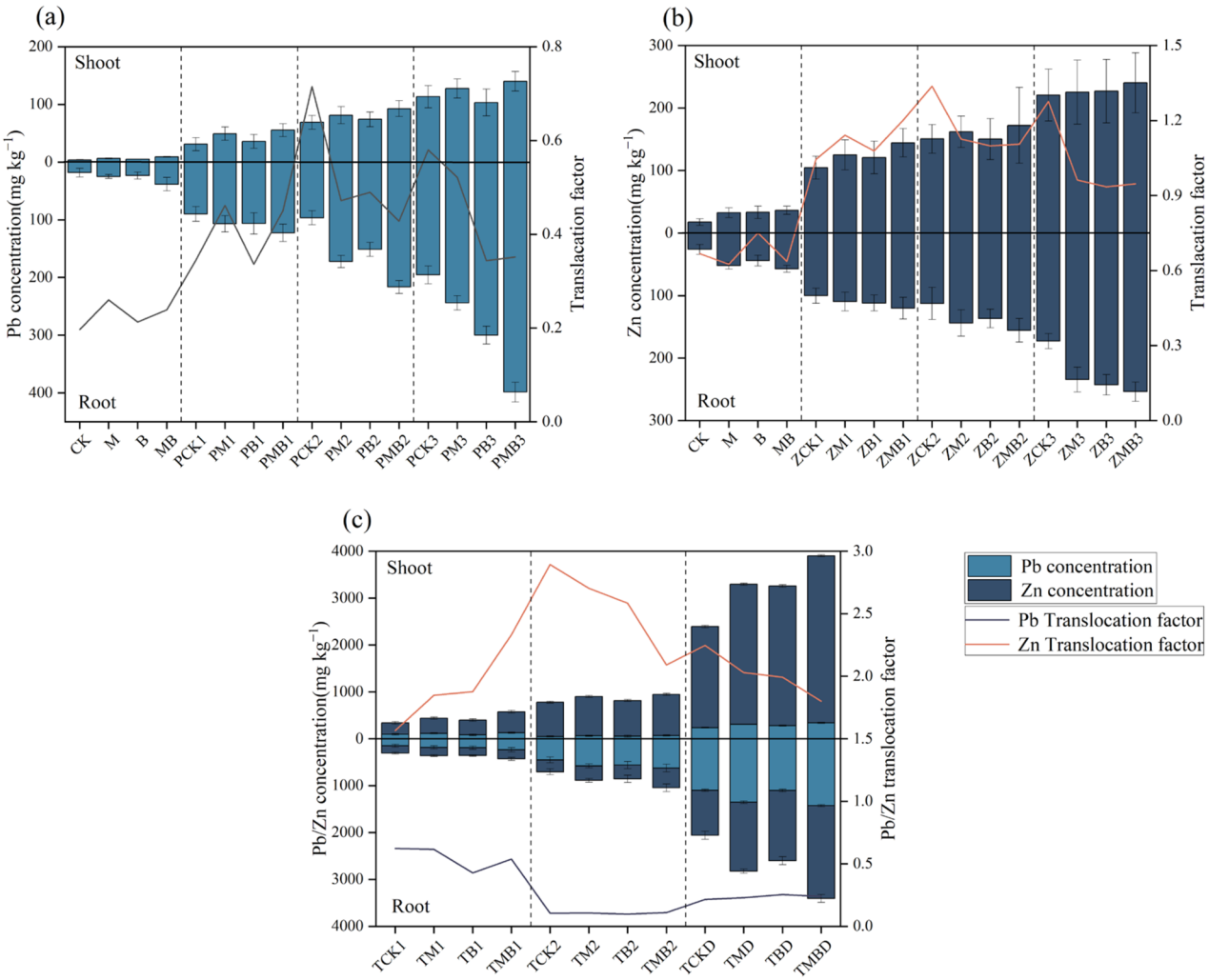

Fig. 4 **a** Pb uptake by castor under Pb stress and transport factors. **b** Zn uptake by castor under Zn stress and transport factors. **c** Accumulation of Pb and Zn by castor under combined Pb and Zn stress and transport factors

transport. Notably, in the treatment group exposed to 300 mg kg^{-1} Pb, the maximum TF index of 71.46% was recorded, whereas TF values in the subsequent treatments decreased to 47.15% (M), 48.95% (B), and 42.79% (MB). This suggests that biochar and multifunctional microbiome treatments rendered castor plants more susceptible to Pb limitation below ground than above ground, a trend observed at Pb concentrations of 300 mg kg^{-1} and higher.

Under Zn stress, the uptake of Zn by plant roots and aboveground parts was comparable (Fig. 4b). When exposed to the same Zn concentration, compared with the control (CK), the application of M and B had little effect on the Zn content in the aboveground part, but increased the Zn content in the underground part. In the treatment group at 800 mg kg^{-1}, the application of M and B increased belowground Zn content by 35.53% and 40.39%, respectively. Notably, the MB treatment was the most effective, resulting in a 46.74% increase in belowground Zn content in castor plants. Overall, the uptake of Zn by plants remained proportional to Zn concentration. At higher Zn concentrations (> 400 mg kg^{-1}), the TF index indicated Zn limitation in the castor, with a subsequent decrease observed in the TF index following M, B, and MB treatments.

Based on the single stress of Pb and Zn, we explored the compound stress of Pb and Zn (Fig. 4c). The uptake of Pb by castor did not show a significant difference compared to the case of single stress. However, the TF index showed a significant ($p < 0.05$) decrease at a particular stage (Pb > 400 mg kg^{-1}), with the highest level of TF index at 25.35% (TBD) and the lowest at 9.84% (TCK2), which suggests that the belowground part of castor was further inhibited under the compound stress, resulting

in decreased transport capacity. The phenomenon that plants showed reduced translocation rates for HMs above a specific concentration indicates that the mobility of HMs in plants is limited (Deng et al. 2004). In contrast, castor showed a fantastic effect on Zn uptake, with aboveground and belowground Zn contents of 3902.67 mg kg^{-1} and 3406.04 mg kg^{-1} in the TMBD group, and the TF indexes exceeded 156%, with a maximum of 289.31%. The significant difference between Pb and Zn may be related to their specific roles in plants, where Zn is involved in protein synthesis, photosynthesis, and plant growth. Zn is involved in some protein synthesis and photosynthesis in plants. At the same time, Pb is not only strongly biotoxic to plants but also inhibits the synthesis and uptake of nutrients in plants (Zhang et al. 2020a). Combining the results of single and compound stresses, similar to the accumulation of Pb and Zn in other plants, Pb is more inclined to accumulate in the roots of plants. At the same time, Zn content is much higher than Pb content in stems, indicating that Zn has a higher mobilizing capacity than Pb (Li et al. 2023c; Zou et al. 2011). It was found that the HM concentration in plants was proportional to the HM concentration in the environment. However, the rate of HM transport from plant roots to stems was reduced, suggesting high plant availability of these HMs (Yang et al. 2021). The significant difference in TF index under compound stress also reveals that castor has a more substantial capacity for Zn uptake and transport.

In conclusion, the utilization of both biochar and multifunctional microbiome effectively augmented the concentrations of Pb and Zn in castor roots and stems. Furthermore, the combined application of these treatments yielded superior outcomes compared to their individual application.

3.3 Impacts on the rhizosphere microenvironment of castor

3.3.1 Effect on bioavailable Pb and Zn of the rhizosphere soil

The bioavailability of HMs is an important indicator for evaluating their plant availability, and their extractable state has a better correlation with soil function, ecotoxicity, and plant absorption (Kumpiene et al. 2014). Under single Pb stress (Fig. 5a), as the treatment concentration increased, the acid-extractable content of Pb generally increased compared with the CK. Under high concentration stress (700 mg kg^{-1}), the acid-extractable Pb content in the MB treatment group was the highest, increasing by 18% compared with CK, followed by the M treatment group, increasing by 15%. Under single Zn stress (Fig. 5b), the acid-extractable Zn content also showed a similar trend. Under high-concentration Zn stress (800 mg kg^{-1}), the M and MB treatment increased the acid-extractable Zn content to 36% and 34%, respectively compared with the CK. Studies have shown that rhizosphere microorganisms can increase the extractable content of HMs by producing organic acids, hyphae chelation, and producing reductases, thereby improving the efficiency of phytoremediation (Jackson et al. 2015; Park et al. 2011; Wu et al. 2006). From the similarity of the trends of Pb and Zn stress, it can be inferred that high concentrations of HM stress will induce the above functions of rhizosphere microorganisms.

Under combined stress (Fig. 5c, d), the acid-extractable contents of Pb and Zn were significantly different among different treatment groups. The effect of biochar on the bioavailability of HMs varies with the type and concentration of metals (Wu et al. 2019), but it shows a good synergistic effect with microorganisms under high-concentration stress. Under high-concentration combined stress (TCKD), the acid-extractable Pb and Zn contents of the MB treatment reached 35% and 30%, respectively, both of which were the highest contents under the same metal types. The results show that under combined stress conditions, the synergistic effect of microorganisms and biochar is most significant. This may be because biochar, as a carrier, provides a safe habitat for microorganisms, and the functional groups between biochar and the microbiome help resist HM stress.

3.3.2 Diversity and structure of rhizosphere soil microbial community

Soil microorganisms are critical components of harmful substances and nutrient transformations in soil (Li et al. 2022). Given the results of Fig. 4, the accumulation of Pb was much higher in the plant below ground than above ground, which was more evident under high concentrations of Pb stress. Therefore, we investigated the effects of different treatments on the diversity of rhizosphere soil microbial communities under high concentrations of Pb stress (700 mg kg^{-1}). From Fig. 6a, it can be found that the composition of the rhizosphere soil microbial community was complex and numerous, and the proportion of the top ten genera in relative abundance to the total sequence was 36.23% on average. It is worth mentioning that *Lactobacillus* appeared in the rhizosphere soil under the M treatment and became the dominant genus under the M treatment group, with a relative abundance of 17.09%. *Lactobacillus* are Gram-positive bacteria that have previously been found to have a wide range of plant growth-promoting properties and can increase the nutrient utilization of compost and other organic materials (Afanador-Barajas et al. 2021). *Lactobacillus* can also remove HMs through electrostatic interactions between HMs and bacterial functional groups (Hasr Moradi Kargar and Hadizadeh Shirazi 2020). We

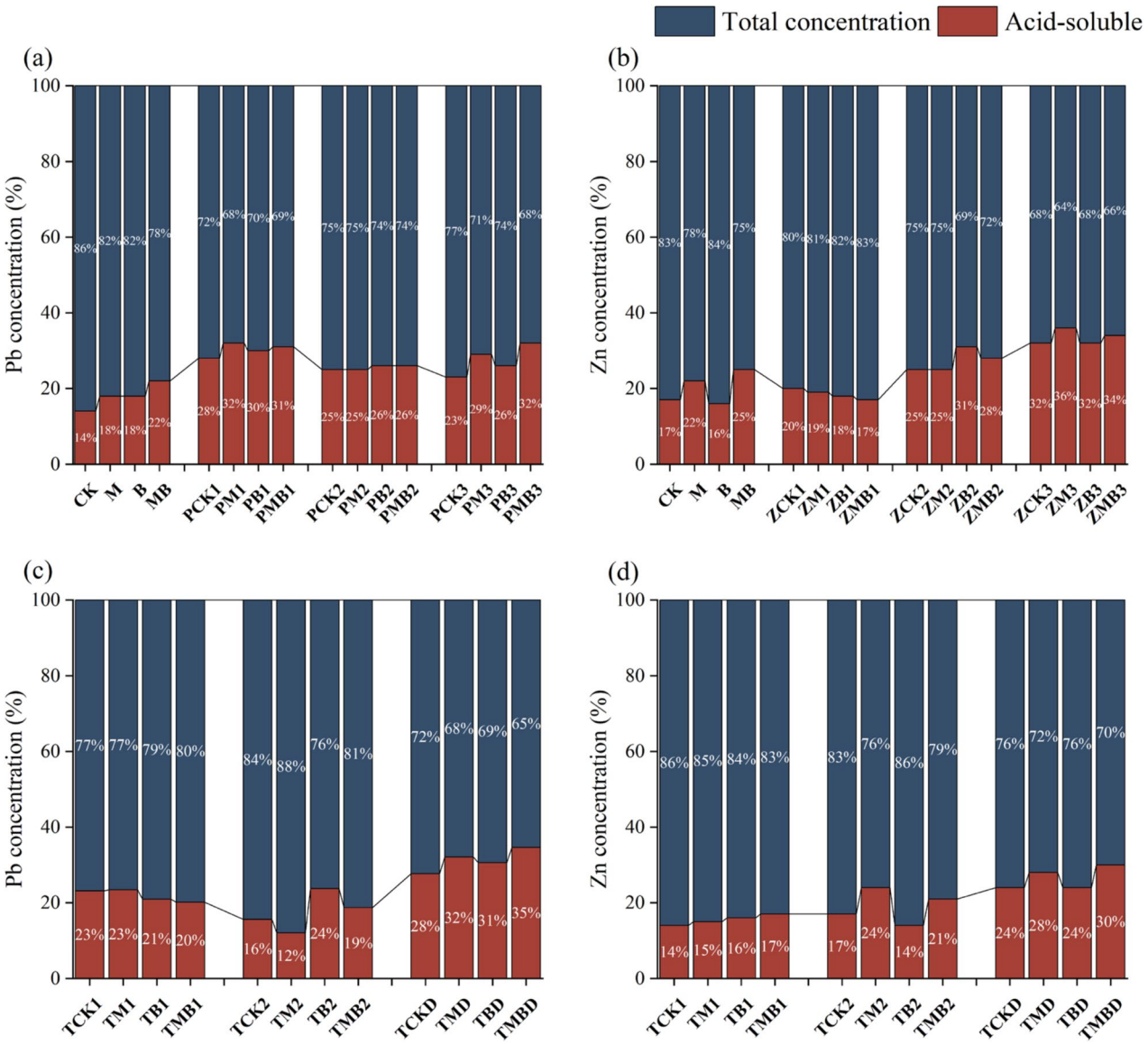

Fig. 5 Percentage of acid-extractable HMs in rhizosphere soil under different treatments. **a** and **b** represent the single stress of Pb and Zn, respectively, **c** and **d** represent the combined stress of Pb and Zn

hypothesize that adding multifunctional microbiome reshaped the soil microbial community composition. At the same time, *Lactobacillus* was increased to fully utilize their phosphorus solubilizing and nitrogen fixing properties to promote plant growth while mitigating Pb stress on plants (Giassi et al. 2016). Meanwhile, the abundance of *Sphingomonas*, *Arthrobacter*, *Sinomonas*, and *Streptomyces* was significantly reduced in the M treatment, accounting for only 2.49% of the total abundance, while in the B and MB treatments, *Arthrobacter*, *Sinomonas* and *Streptomyces* were not significantly different from those in CK, while *Sphingomonas* increased its abundance by 11.71% under B treatment.

Figure 6b illustrates the variability in the relative abundance of the top ten fungal genera across different treatments of Pb-contaminated soil. The predominant genera in each treatment included *Aspergillus*, *Cladosporium*, *Alternaria*, *Saitozyma*, and *Candida*, collectively constituting over 56.38% of the total sequences, with the most abundant genus representing 73.80% of the total sequences. Notably, significant differences were observed in the relative abundance of dominant genera among

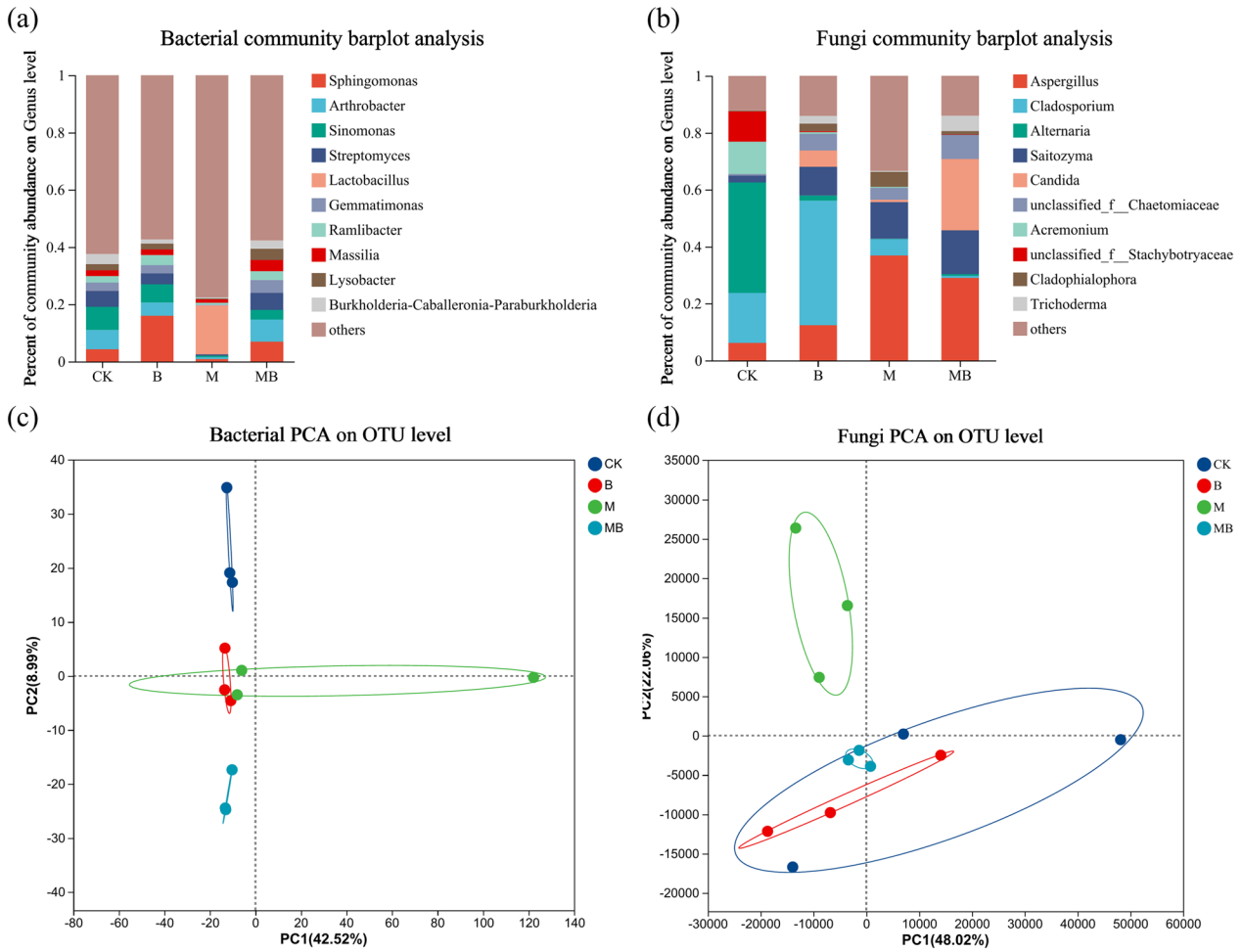

Fig. 6 Principal component analysis of bacterial community (**a**) and fungal community (**b**) as well as bacterial (**c**) and fungal (**d**) communities in rhizosphere microorganisms under Pb stress (700 mg kg^{-1}). Where PC1 and PC2 represent the two selected principal component axes, and the percentage indicates the value of the degree of explanation of differences in sample composition by the principal component

soils treated differently, with a notable feature being the variation in dominant genera across treatments. *Alternaria*, the dominant genus in the CK treatment (comprising 38.80% abundance), exhibited a substantial decrease of 37.10% in abundance in the B treatment, and its abundance was completely absent in the M and MB treatments.

Meanwhile, *Cladosporium* significantly increased its abundance by 26.15% in the B treatment and became the dominant genus with 43.74% abundance in the B treatment. In contrast, in the M and MB treatments, it was the dominant genus in the B treatment. The dominant genus significantly decreased by 11.80% and 16.83% under M and MB treatments. The average increase in abundance of *Saitozyma* was 10.33% under B, M, and MB treatments, with insignificant differences between groups; the relative abundance of *Aspergillus* significantly increased by 30.80% and 22.86% under M and MB treatments, respectively, and became the dominant genus in the M and MB groups. The function of a fungal community is not the sum of its components but the result of the interaction of each component with the plant (Sun et al. 2022). *Aspergillus* is one of the most common genera of soil fungi, which is remarkably tolerant to highly stressful environments. While *Aspergillus* can secrete amylases, xylanases, and pectinases to degrade polymers in the substrate into molecules that can be taken up as nutrients (Krijgsheld et al. 2013; Nji et al. 2023). The increase in the abundance of *Aspergillus* may be related to the nutrient enrichment of the soil after the addition of biochar.

Plant-associated rhizosphere microbial communities reveal more fully the effects of different treatments of plants on HM remediation. PCA analysis revealed the effects of different treatments on microbial community structure. Axes PC1 and PC2 explained 51.51% of the total variation in bacterial community composition and

70.08% of the total variation in fungal community composition (Fig. 6c, d). Bacterial communities showed different clustering patterns under different treatments, with denser aggregations in the M, B, and MB treatments compared to the control. From Fig. 6d, MB treatment appeared to stably affect the microbial community structure and reduce intra-group differences compared to the control. It is worth noting that despite differences in microbial community composition at the genus level among the treatment groups, there was overlap in the PCA results due to the similarity of some features on the principal component axes. Figure 6 shows that MB treatment can effectively reduce the differences in soil microbial communities and make the structure of soil microbial communities stable. We believe that there are two reasons for such a significant effect of MB treatment: on the one hand, the sludge biochar changed the soil nutrient system, which altered the original soil ecological balance; on the other hand, the introduction of multifunctional microbiome altered the homogeneity and abundance of the original soil microbial community, and formed a new equilibrium (He et al. 2022; Song et al. 2021).

3.3.3 Functional prediction of bacterial and fungal communities in soil

To better understand the microecological functions of microorganisms in the rhizosphere soil of castor, we used PICRUSt2 to predict the functional composition of the bacterial community (Fig. 7a). Based on the COG database, we compared sequencing data and performed direct functional annotation of sequenced genomes (Galperin et al. 2019). Bacterial COG functional categorization showed that among the 23 categories of COG functional annotation results (Figure S3), there was a wide variety of metabolism-related functions, including amino acid transport and metabolism, energy production and conversion, translation, ribosomal

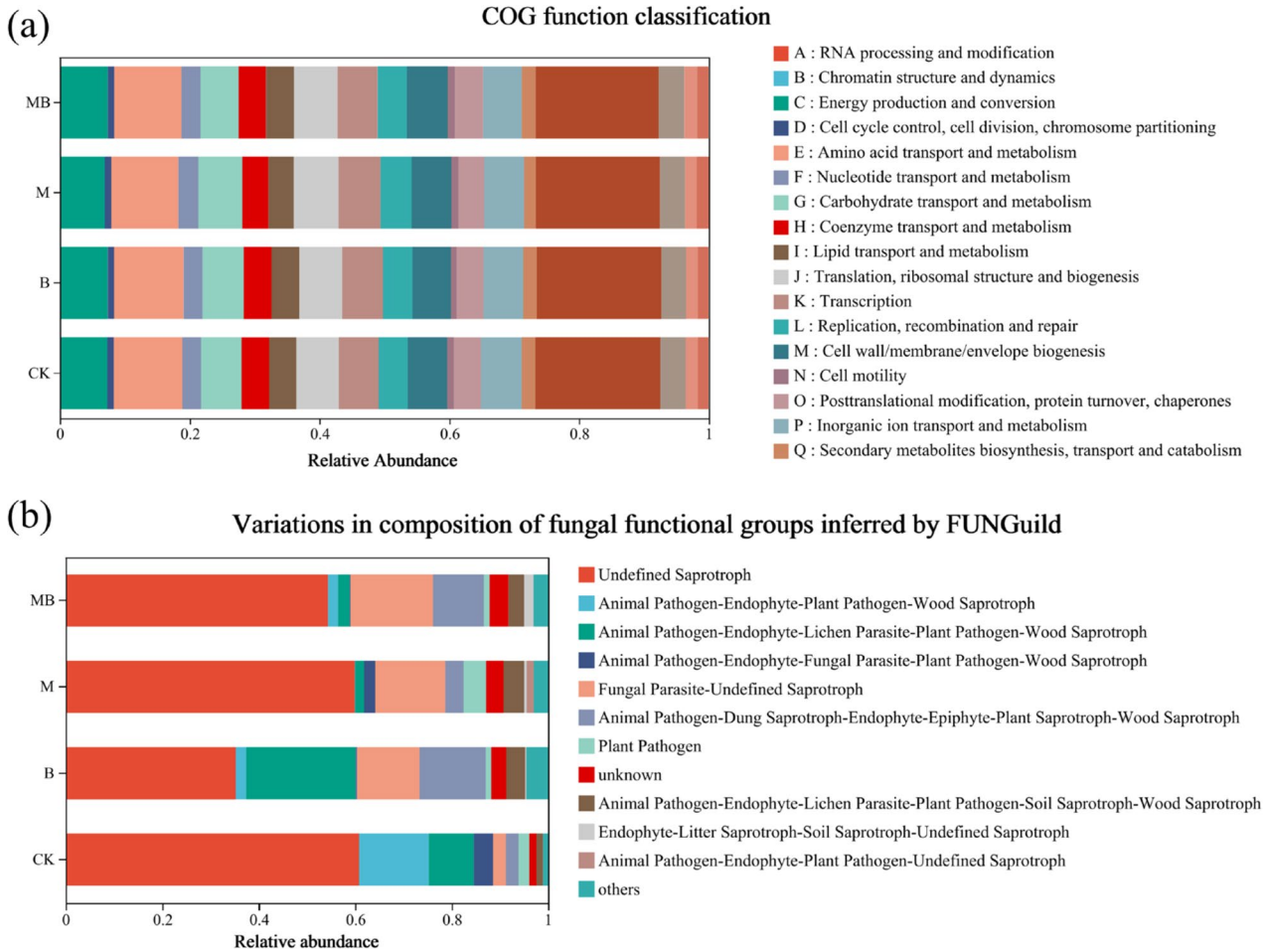

Fig. 7 Functional characteristics of microbial communities in castor soil under Pb stress (700 mg kg^{-1}) in different treatments. **a** Functional characteristics of bacterial community and **b** functional characteristics of fungal community. Horizontal coordinates represent COG functional classification and vertical coordinates represent functional abundance

structure and biogenesis, carbohydrate transport and metabolism, transcription, inorganic ion transport, and metabolism, cell wall/membrane/envelope biogenesis. All sample loci in the COG analysis were associated with having a similar enrichment function related to bacterial community structure. The relative functional abundance of the main functional characteristics of the bacterial community was highest under the B treatment and lowest under the M treatment. The M treatment promotes specific functional characteristics within the bacterial community, highlighting its targeted impact compared to broader enhancements seen with biochar.

Next, the function of the fungal community was predicted using FUNGuild analysis (Fig. 7b), based on which information on the functional classifications of the fungi in the samples and the abundance of each functional classification in different samples could be obtained. The OTUs of fungi were classified based on different nutritional modes and further classified by how fungi take on the uptake and utilization of environmental resources. The relative abundance of Undefined Saprotroph was dominant in all four treatment species, followed by Animal Pathogen-Endophyte-Plant Pathogen-Wood Saprotroph (CK, 14.45%), Animal Pathogen-Endophyte-Lichen Parasite-Plant Pathogen-Wood Saprotroph (B, 22.72%), and Fungal Parasite-Undefined Saprotroph (M,14.61%; MB,17.10%). This result indicates that the trophic pattern of the castor's dominant rhizosphere fungal community differed in different treatments. Out of 792 fungal OTUs, 31 had highly probable confidence rankings. These OTUs with high confidence belonged to four trophic modes: saprotroph (48.39%), symbiotroph (45.16%), pathotroph (0.03%), pathotroph-saprotroph (0.03%). Furthermore, most of these symbiotrophs were composed of clumping mycorrhizal fungi (57.14%). Clumping mycorrhizal fungi are associated with more than 80% of terrestrial plant species due to their ability to form extensive mycelial networks that help plants absorb nutrients from the soil (Armada 2017; Cao et al. 2022b). In soil ecosystems, saprotrophic fungi play an essential role in organic matter decomposition, carbon cycling, nutrient mobilization, and the creation of soil structure (Schmidt et al. 2019). Previous studies have demonstrated that AMF will colonize in the presence of saprotrophic fungi, absorbing nutrients from plant litter and to the host plant while indirectly stimulating the decomposition of organic matter by saprotrophic bacteria (Cao et al. 2022b). In this study, the abundance of saprotroph decreased in B and MB treatments after the introduction of the multifunctional microbiome, indicating that the original microbial community of the soil was changed. At the same time, the nutritional mode of the microbial community was also adjusted.

4 Conclusion

In this study, sludge biochar was confirmed to be an effective microbial carrier, and the composite microbial agent prepared from it can effectively improve the phytoremediation efficiency. Castor demonstrated efficient aboveground Zn transport in simulated remediation experiments. At the same time, phenotypic damage to plant roots caused by natural slag was observed under conditions of high-level composite stress, whereas, the synergistic effects of MB treatment significantly enhanced root morphological parameters and the uptake of Pb and Zn, indicating their positive impact on plant growth and metal absorption. From a microscopic perspective, the microbiome boosted abundance of PGPRs to promote plant growth and resist HM stress. In summary, the combination of sludge biochar and microbiome provides a novel approach to remediate HMs in soil.

Supplementary Information

The online version contains supplementary material available at https://doi.org/10.1007/s42773-024-00395-2.

Supplementary Material 1.

Acknowledgements

The corresponding author would like to acknowledge the National Natural Science Foundation of China (32201394, 51709285), Chenzhou National Sustainable Development Project (2022sfq53), Hunan Key Research and Development Project (2023SK2078), Hunan Forestry Science and Technology Plan Project (XLK202449), Science and Technology Planning Project of Hunan Province (2022RC4031), Hunan Natural Science Foundation (2023JJ10023), Hunan Province Natural Resources Science and Technology Plan Project (20230137ST).

Author contributions

Zihao Yang: investigation, formal analysis, writing—original draft. Lijuan Jiang: investigation, resources. Xuejun Li: software, data curation, visualization. Qiaoling Ji: data curation, funding acquisition. Mengyuan Wang: data curation. Yi Zhang, Yuanlin Cheng: writing—review and editing. Xuan Zhang, Hui Li, Chongling Feng: conceptualization, supervision, writing—review and editing. All authors read and approved the final manuscript.

Funding

This work was financially supported by National Natural Science Foundation of China (32201394, 51709285), Chenzhou National Sustainable Development Project (2022sfq53), Hunan Key Research and Development Project (2023SK2078), Hunan Forestry Science and Technology Plan Project (XLK202449), Science and Technology Planning Project of Hunan Province (2022RC4031), Hunan Natural Science Foundation (2023JJ10023), Hunan Province Natural Resources Science and Technology Plan Project (20230137ST).

Data availability

The datasets utilized or analyzed during this study are available from the corresponding author upon reasonable request.

Declarations

Competing interests

Authors declare no conflict of interest either financially or otherwise.

Author details

[1]College of Life and Environmental Sciences, Central South University of Forestry and Technology, Changsha 410004, Hunan, China. [2]State Key Laboratory of Utilization of Woody Oil Resource, Hunan Academy of Forestry, Changsha 410004, Hunan, China. [3]China Energy Engineering Group Hunan Electric Power Design Institute Co., LTD, Changsha 410000, Hunan, China.

Received: 28 April 2024 Revised: 11 October 2024 Accepted: 18 October 2024
Published online: 02 January 2025

References

Abedi T, Gavanji S, Mojiri A (2022) Lead and zinc uptake and toxicity in maize and their management. Plants. https://doi.org/10.3390/plants11151922

Adesemoye AO, Torbert HA, Kloepper JW (2009) Plant growth-promoting rhizobacteria allow reduced application rates of chemical fertilizers. Microb Ecol 58(4):921–929. https://doi.org/10.1007/s00248-009-9531-y

Afanador-Barajas LN, Navarro-Noya YE, Luna-Guido ML, Dendooven L (2021) Impact of a bacterial consortium on the soil bacterial community structure and maize (*Zea mays* L.) cultivation. Sci Rep 11(1):13092. https://doi.org/10.1038/s41598-021-92517-0

Afonso TF, Demarco CF, Pieniz S, Camargo FAO, Quadro MS, Andreazza R (2019) Potential of *Solanum viarum* Dunal in use for phytoremediation of heavy metals to mining areas, southern Brazil. Environ Sci Pollut Res Int 26(23):24132–24142. https://doi.org/10.1007/s11356-019-05460-z

Ali H, Khan E, Sajad MA (2013) Phytoremediation of heavy metals—concepts and applications. Chemosphere 91(7):869–881. https://doi.org/10.1016/j.chemosphere.2013.01.075

Aloni R, Aloni E, Langhans M, Ullrich CI (2006) Role of cytokinin and auxin in shaping root architecture: regulating vascular differentiation, lateral root initiation, root apical dominance and root gravitropism. Ann Bot 97(5):883–893. https://doi.org/10.1093/aob/mcl027

Anwar S, Ali B, Sajid I (2016) Screening of rhizospheric actinomycetes for various in-vitro and in-vivo plant growth promoting (PGP) traits and for agroactive compounds. Front Microbiol 7:1334. https://doi.org/10.3389/fmicb.2016.01334

Arasu MV, Duraipandiyan V, Ignacimuthu S (2013) Antibacterial and antifungal activities of polyketide metabolite from marine *Streptomyces* sp. AP-123 and its cytotoxic effect. Chemosphere 90(2):479–487. https://doi.org/10.1016/j.chemosphere.2012.08.006

Armada E, López-Castillo O, Roldán A, Azcón R (2017) Potential of mycorrhizal inocula to improve growth, nutrition and enzymatic activities in *Retama sphaerocarpa* compared with chemical fertilization under drought conditions. SIAM J Appl Dyn Syst 16(2):380

Bauddh K, Singh K, Singh B, Singh RP (2015) *Ricinus communis*: a robust plant for bio-energy and phytoremediation of toxic metals from contaminated soil. Ecol Eng 84:640–652. https://doi.org/10.1016/j.ecoleng.2015.09.038

Baudy P, Zubrod JP, Konschak M, Kolbenschlag S, Pollitt A, Baschien C, Schulz R, Bundschuh M (2021) Fungal–fungal and fungal–bacterial interactions in aquatic decomposer communities: bacteria promote fungal diversity. Ecology 102(10):e03471. https://doi.org/10.1002/ecy.3471

Beneduzi A, Ambrosini A, Passaglia LM (2012) Plant growth-promoting rhizobacteria (PGPR): their potential as antagonists and biocontrol agents. Genet Mol Biol 35(4 Suppl 1):1044–1051. https://doi.org/10.1590/s1415-47572012000600020

Bertrand S, Bohni N, Schnee S, Schumpp O, Gindro K, Wolfender JL (2014) Metabolite induction via microorganism co-culture: a potential way to enhance chemical diversity for drug discovery. Biotechnol Adv 32(6):1180–1204. https://doi.org/10.1016/j.biotechadv.2014.03.001

Boratyn GM, Camacho C, Cooper PS, Coulouris G, Fong A, Ma N, Madden TL, Matten WT, McGinnis SD, Merezhuk Y, Raytselis Y, Sayers EW, Tao T, Ye J, Zaretskaya I (2013) BLAST: a more efficient report with usability improvements. Nucl Acids Res 41(Web Server):W29-33. https://doi.org/10.1093/nar/gkt282

Cai LM, Wang QS, Luo J, Chen LG, Zhu RL, Wang S, Tang CH (2019) Heavy metal contamination and health risk assessment for children near a large Cu-smelter in central China. Sci Total Environ 650(Pt 1):725–733. https://doi.org/10.1016/j.scitotenv.2018.09.081

Cao J, Xie CY, Hou ZR (2022a) Ecological evaluation of heavy metal pollution in the soil of Pb-Zn mines. Ecotoxicology 31(2):259–270. https://doi.org/10.1007/s10646-021-02505-3

Cao TT, Fang Y, Chen YR, Kong XS, Yang JB, Alharbi H, Kuzyakov Y, Tian XJ (2022b) Synergy of saprotrophs with mycorrhiza for litter decomposition and hotspot formation depends on nutrient availability in the rhizosphere. Geoderma. https://doi.org/10.1016/j.geoderma.2021.115662

Chen HM, Zhang JW, Tang LY, Su M, Tian D, Zhang L, Li Z, Hu SJ (2019) Enhanced Pb immobilization via the combination of biochar and phosphate solubilizing bacteria. Environ Int 127:395–401. https://doi.org/10.1016/j.envint.2019.03.068

Chen YD, Wang R, Duan X, Wang S, Ren NQ, Ho SH (2020) Production, properties, and catalytic applications of sludge derived biochar for environmental remediation. Water Res 187:116390. https://doi.org/10.1016/j.watres.2020.116390

Chen L, Zhang X, Zhang M, Zhu Y, Zhuo R (2022) Removal of heavy-metal pollutants by white rot fungi: mechanisms, achievements, and perspectives. J Clean Prod 354:131681

Chen S, Zhong M, Wang H, Zhou S, Li W, Wang T, Li J (2023) Study on adsorption of Cu^{2+}, Pb^{2+}, Cd^{2}+, and Zn^{2+} by the $KMnO_4$ modified biochar derived from walnut shell. Int J Environ Sci Technol 20(2):1551–1568

de Figueiredo CC, Farias WM, Coser TR, Monteiro de Paula A, Sartori da Silva MR, Paz-Ferreiro J (2019) Sewage sludge biochar alters root colonization of mycorrhizal fungi in a soil cultivated with corn. Eur J Soil Biol. https://doi.org/10.1016/j.ejsobi.2019.103092

Deng H, Ye ZH, Wong MH (2004) Accumulation of lead, zinc, copper and cadmium by 12 wetland plant species thriving in metal-contaminated sites in China. Environ Pollut 132(1):29–40. https://doi.org/10.1016/j.envpol.2004.03.030

Deng SX, Zhang X, Zhu YH, Zhuo R (2024) Recent advances in phyto-combined remediation of heavy metal pollution in soil. Biotechnol Adv 72:108337. https://doi.org/10.1016/j.biotechadv.2024.108337

Etesami H, Jeong BR, Glick BR (2021) Contribution of arbuscular mycorrhizal fungi, phosphate-solubilizing bacteria, and silicon to P uptake by plant. Front Plant Sci 12:699618. https://doi.org/10.3389/fpls.2021.699618

Fahr M, Laplaze L, Bendaou N, Hocher V, Mzibri ME, Bogusz D, Smouni A (2013) Effect of lead on root growth. Front Plant Sci 4:175

Fan MC, Liu ZS, Nan LJ, Wang ET, Chen WM, Lin YB, Wei GH (2018) Isolation, characterization, and selection of heavy metal-resistant and plant growth-promoting endophytic bacteria from root nodules of *Robinia pseudoacacia* in a Pb/Zn mining area. Microbiol Res 217:51–59. https://doi.org/10.1016/j.micres.2018.09.002

Fan H, Huang Z, Feng C, Wu Z, Tian Y, Ma F, Li H, Huang J, Qin X, Zhou Z (2024) Functional keystone taxa promote N and P removal of the constructed wetland to mitigate agricultural nonpoint source pollution. Sci Total Environ 912:169155

Galperin MY, Kristensen DM, Makarova KS, Wolf YI, Koonin EV (2019) Microbial genome analysis: the COG approach. Brief Bioinform 20(4):1063–1070. https://doi.org/10.1093/bib/bbx117

Ghahremani M, MacLean AM (2021) Home sweet home: how mutualistic microbes modify root development to promote symbiosis. J Exp Bot 72(7):2275–2287. https://doi.org/10.1093/jxb/eraa607

Ghosh D, Maiti SK (2021) Biochar assisted phytoremediation and biomass disposal in heavy metal contaminated mine soils: a review. Int J Phytoremediation 23(6):559–576

Giassi V, Kiritani C, Kupper KC (2016) Bacteria as growth-promoting agents for citrus rootstocks. Microbiol Res 190:46–54. https://doi.org/10.1016/j.micres.2015.12.006

Glick BR, Todorovic B, Czarny J, Cheng Z, Duan J, McConkey B (2007) Promotion of plant growth by bacterial ACC deaminase. Crit Rev Plant Sci 26(5–6):227–242. https://doi.org/10.1080/07352680701572966

Goswami D, Thakker JN, Dhandhukia PC (2016) Portraying mechanics of plant growth promoting rhizobacteria (PGPR): a review. Cogent Food Agric 2(1):1127500

Hannula SE, Morrien E, de Hollander M, van der Putten WH, van Veen JA, de Boer W (2017) Shifts in rhizosphere fungal community during secondary succession following abandonment from agriculture. ISME J 11(10):2294–2304. https://doi.org/10.1038/ismej.2017.90

Hasr Moradi Kargar S, Hadizadeh Shirazi N (2020) *Lactobacillus fermentum* and *Lactobacillus plantarum* bioremediation ability assessment for copper and zinc. Arch Microbiol 202(7):1957–1963. https://doi.org/10.1007/s00203-020-01916-w

He CQ, Zhao YP, Wang FF, Oh K, Zhao ZZ, Wu CL, Zhang XY, Chen XP, Liu XY (2020) Phytoremediation of soil heavy metals (Cd and Zn) by castor seedlings: tolerance, accumulation and subcellular distribution. Chemosphere 252:126471. https://doi.org/10.1016/j.chemosphere.2020.126471

He YQ, Wang HM, Liu Y, Zuo MB, Wang XY, Shen YY, Li GW, Hu YN, Zhao MJ, Yang YL, Zhao YY, Gao TP (2022) Distribution and variation of soil bacterial community of two lead-zinc tailings in qinling mountains. Geomicrobiol J 40(1):1–11. https://doi.org/10.1080/01490451.2022.2124330

Hibbing ME, Fuqua C, Parsek MR, Peterson SB (2010) Bacterial competition: surviving and thriving in the microbial jungle. Nat Rev Microbiol 8(1):15–25. https://doi.org/10.1038/nrmicro2259

Jackson TA, Vlaar S, Nguyen N, Leppard GG, Finan TM (2015) Effects of bioavailable heavy metal species, arsenic, and acid drainage from mine tailings on a microbial community sampled along a pollution gradient in a freshwater ecosystem. Geomicrobiol J 32(8):724–750

Ji XW, Wan J, Wang XD, Peng C, Wang GH, Liang WY, Zhang W (2022) Mixed bacteria-loaded biochar for the immobilization of arsenic, lead, and cadmium in a polluted soil system: effects and mechanisms. Sci Total Environ 811:152112. https://doi.org/10.1016/j.scitotenv.2021.152112

Joseph S, Cowie AL, Zwieten LV, Bolan N, Lehmann J (2021) How biochar works, and when it doesn't: a review of mechanisms controlling soil and plant responses to biochar. GCB Bioenergy. https://doi.org/10.1111/gcbb.12885

Kaur H, Garg N (2021) Zinc toxicity in plants: a review. Planta 253(6):129

Khan N, Bano A, Ali S, Babar MA (2020) Crosstalk amongst phytohormones from planta and PGPR under biotic and abiotic stresses. Plant Growth Regul 90(2):189–203. https://doi.org/10.1007/s10725-020-00571-x

Kiran BR, Prasad MNV (2019) Biochar and rice husk ash assisted phytoremediation potentials of *Ricinus communis* L. for lead—spiked soils. Ecotoxicol Environ Saf 183:109574. https://doi.org/10.1016/j.ecoenv.2019.109574

Kizilkaya R (2009) Nitrogen fixation capacity of *Azotobacter* spp. strains isolated from soils in different ecosystems and relationship between them and the microbiological properties of soils. J Environ Biol 30(1):73–82

Krijgsheld P, Bleichrodt R, van Veluw GJ, Wang F, Muller WH, Dijksterhuis J, Wosten HA (2013) Development in *Aspergillus*. Stud Mycol 74(1):1–29. https://doi.org/10.3114/sim0006

Kumpiene J, Bert V, Dimitriou I, Eriksson J, Friesl-Hanl W, Galazka R, Herzig R, Janssen J, Kidd P, Mench M (2014) Selecting chemical and ecotoxicological test batteries for risk assessment of trace element-contaminated soils (phyto) managed by gentle remediation options (GRO). Sci Total Environ 496:510–522

Lai-Guo C, Yong R (2004) Recent advances in phyto-remediation of soil contamination by polycyclic aromatic hydrocarbons. Environ Sci Technol. https://doi.org/10.1021/acs.estlett.0c00677

Li PH, Lin CY, Cheng HG, Duan XL, Lei K (2015) Contamination and health risks of soil heavy metals around a lead/zinc smelter in southwestern China. Ecotoxicol Environ Saf 113:391–399. https://doi.org/10.1016/j.ecoenv.2014.12.025

Li XG, Garbeva P, Liu XJ, Klein Gunnewiek PJA, Clocchiatti A, Hundscheid MPJ, Wang XX, de Boer W (2020) Volatile-mediated antagonism of soil bacterial communities against fungi. Environ Microbiol 22(3):1025–1035. https://doi.org/10.1111/1462-2920.14808

Li JH, Xia CG, Cheng R, Lan JR, Chen FY, Li XL, Li SY, Chen JA, Zeng TY, Hou HB (2022) Passivation of multiple heavy metals in lead-zinc tailings facilitated by straw biochar-loaded N-doped carbon aerogel nanoparticles: mechanisms and microbial community evolution. Sci Total Environ 803:149866. https://doi.org/10.1016/j.scitotenv.2021.149866

Li MY, Chen XT, Chen CY, Huang LG, Chi HC, Zhao N, Yan BF, Chao YQ, Tang YT, Qiu RL, Wang SZ (2023a) The effectiveness of sewage sludge biochar amendment with *Boehmeria nivea* L. in improving physicochemical properties and rehabilitating microbial communities in mine tailings. J Environ Manag 345:118552. https://doi.org/10.1016/j.jenvman.2023.118552

Li X, Zeng J, Zuo S, Lin S, Chen G (2023b) Preparation, modification, and application of biochar in the printing field: a review. Materials. https://doi.org/10.3390/ma16145081

Li Y, Wang C, Yan C, Liu S, Chen X, Zeng M, Dong Y, Jiao R (2023c) Heavy metal concentrations and accumulation characteristics of dominant woody plants in iron and lead-zinc tailing areas in Jiangxi, southeast China. Forests. https://doi.org/10.3390/f14040846

Li Y, Chen Y, Fu Y, Shao J, Liu Y, Xuan W, Xu G, Zhang R (2024) Signal communication during microbial modulation of root system architecture. J Exp Bot 75(2):526–537. https://doi.org/10.1093/jxb/erad263

Liu GN, Wang J, Liu X, Liu XH, Li XS, Ren YQ, Wang J, Dong LM (2018) Partitioning and geochemical fractions of heavy metals from geogenic and anthropogenic sources in various soil particle size fractions. Geoderma 312:104–113. https://doi.org/10.1016/j.geoderma.2017.10.013

Lobo LLB, de Andrade da Silva MSR, Castellane TCL, Carvalho RF, Rigobelo EC (2022) Effect of indole-3-acetic acid on tomato plant growth. Microorganisms. https://doi.org/10.3390/microorganisms10112212

Lugtenberg B, Kamilova F (2009) Plant-growth-promoting rhizobacteria. Annu Rev Microbiol 63:541–556. https://doi.org/10.1146/annurev.micro.62.081307.162918

Luo X, Wu C, Lin Y, Li W, Deng M, Tan J, Xue S (2023) Soil heavy metal pollution from Pb/Zn smelting regions in China and the remediation potential of biomineralization. J Environ Sci 125:662–677. https://doi.org/10.1016/j.jes.2022.01.029

Mille-Lindblom C, Tranvik LJ (2003) Antagonism between bacteria and fungi on decomposing aquatic plant litter. Microb Ecol 45(2):173–182. https://doi.org/10.1007/s00248-002-2030-z

Nautiyal CS (1999) An efficient microbiological growth medium for screening phosphate solubilizing microorganisms. FEMS Microbiol Lett 170(1):265–270. https://doi.org/10.1111/j.1574-6968.1999.tb13383.x

Nji QN, Babalola OO, Mwanza M (2023) Soil *Aspergillus* species, pathogenicity and control perspectives. J Fungi. https://doi.org/10.3390/jof9070766

Park JH, Bolan N, Megharaj M, Naidu R (2011) Concomitant rock phosphate dissolution and lead immobilization by phosphate solubilizing bacteria (*Enterobacter* sp.). J Environ Manag 92(4):1115–1120

Peng JY, Zhang S, Han Y, Bate B, Ke H, Chen Y (2022) Soil heavy metal pollution of industrial legacies in China and health risk assessment. Sci Total Environ 816:151632. https://doi.org/10.1016/j.scitotenv.2021.151632

Penrose DM, Glick BR (2003) Methods for isolating and characterizing ACC deaminase-containing plant growth-promoting rhizobacteria. Physiol Plant 118(1):10–15. https://doi.org/10.1034/j.1399-3054.2003.00086.x

Schmidt R, Mitchell J, Scow K (2019) Cover cropping and no-till increase diversity and symbiotroph:saprotroph ratios of soil fungal communities. Soil Biol Biochem 129:99–109. https://doi.org/10.1016/j.soilbio.2018.11.010

Shahzad R, Waqas M, Khan AL, Al-Hosni K, Kang SM, Seo CW, Lee IJ (2017) Indoleacetic acid production and plant growth promoting potential of bacterial endophytes isolated from rice (*Oryza sativa* L.) seeds. Acta Biol Hung 68(2):175–186. https://doi.org/10.1556/018.68.2017.2.5

Simmer RA, Schnoor JL (2022) Phytoremediation, bioaugmentation, and the plant microbiome. Environ Sci Technol 56(23):16602–16610. https://doi.org/10.1021/acs.est.2c05970

Singh S, Kumar V, Dhanjal DS, Datta S, Bhatia D, Dhiman J, Samuel J, Prasad R, Singh J (2020) A sustainable paradigm of sewage sludge biochar: valorization, opportunities, challenges and future prospects. J Clean Prod 269:122259. https://doi.org/10.1016/j.jclepro.2020.122259

Song A, Li Z, Wang E, Xu D, Wang S, Bi J, Wang H, Jeyakumar P, Li Z, Fan F (2021) Supplying silicon alters microbial community and reduces soil cadmium bioavailability to promote health wheat growth and yield. Sci Total Environ 796:148797. https://doi.org/10.1016/j.scitotenv.2021.148797

Soumare A, Diedhiou AG, Thuita M, Hafidi M, Ouhdouch Y, Gopalakrishnan S, Kouisni L (2020) Exploiting biological nitrogen fixation: a route towards a sustainable agriculture. Plants. https://doi.org/10.3390/plants9081011

Spaepen S, Vanderleyden J, Remans R (2007) Indole-3-acetic acid in microbial and microorganism-plant signaling. FEMS Microbiol Rev 31(4):425–448. https://doi.org/10.1111/j.1574-6976.2007.00072.x

Sun R, Yi Z, Fu Y, Liu H (2022) Dynamic changes in rhizosphere fungi in different developmental stages of wheat in a confined and isolated environment. Appl Microbiol Biotechnol 106(1):441–453. https://doi.org/10.1007/s00253-021-11698-w

Suo Y, Tang N, Li H, Corti G, Jiang L, Huang Z, Zhang Z, Huang J, Wu Z, Feng C, Zhang X (2021) Long-term effects of phytoextraction by a poplar clone

on the concentration, fractionation, and transportation of heavy metals in mine tailings. Environ Sci Pollut Res Int 28(34):47528–47539. https://doi.org/10.1007/s11356-021-13864-z
Thijs S, Sillen W, Weyens N, Vangronsveld J (2017) Phytoremediation: State-of-the-art and a key role for the plant microbiome in future trends and research prospects. Int J Phytoremediation 19(1):23–38. https://doi.org/10.1080/15226514.2016.1216076
Tian Y, Li J, McGill WB, Whitcombe TW (2021) Impact of pyrolysis temperature and activation on oily sludge–derived char for Pb (II) and Cd (II) removal from aqueous solution. Environ Sci Pollut Res 28:5532–5547
Vacheron J, Desbrosses G, Bouffaud M-L, Touraine B, Moënne-Loccoz Y, Muller D, Legendre L, Wisniewski-Dyé F, Prigent-Combaret C (2013) Plant growth-promoting rhizobacteria and root system functioning. Front Plant Sci 4:356
van Loon LC (2007) Plant responses to plant growth-promoting rhizobacteria. Eur J Plant Pathol 119(3):243–254. https://doi.org/10.1007/s10658-007-9165-1
Wang J, Wang S (2019) Preparation, modification and environmental application of biochar: a review. J Clean Prod 227:1002–1022. https://doi.org/10.1016/j.jclepro.2019.04.282
Wang L, Ji B, Hu Y, Liu R, Sun W (2017) A review on in situ phytoremediation of mine tailings. Chemosphere 184:594–600. https://doi.org/10.1016/j.chemosphere.2017.06.025
Wang X, Zhang X, Liu X, Huang Z, Niu S, Xu T, Zeng J, Li H, Wang T, Gao Y, Huang M, Cao L, Zhu Y (2019) Physiological, biochemical and proteomic insight into integrated strategies of an endophytic bacterium *Burkholderia cenocepacia* strain YG-3 response to cadmium stress. Metallomics 11(7):1252–1264. https://doi.org/10.1039/c9mt00054b
Wang R, Duan X, Wang S, Ren N-Q, Ho S-H (2020) Production, properties, and catalytic applications of sludge derived biochar for environmental remediation. Water Res 187:116390
Wiegand I, Hilpert K, Hancock RE (2008) Agar and broth dilution methods to determine the minimal inhibitory concentration (MIC) of antimicrobial substances. Nat Protoc 3(2):163–175. https://doi.org/10.1038/nprot.2007.521
Wu S, Luo Y, Cheung K, Wong MH (2006) Influence of bacteria on Pb and Zn speciation, mobility and bioavailability in soil: a laboratory study. Environ Pollut 144(3):765–773
Wu B, Wang Z, Zhao Y, Gu Y, Wang Y, Yu J, Xu H (2019) The performance of biochar-microbe multiple biochemical material on bioremediation and soil micro-ecology in the cadmium aged soil. Sci Total Environ 686:719–728
Xia Z, Zhang S, Cao Y, Zhong Q, Wang G, Li T, Xu X (2019) Remediation of cadmium, lead and zinc in contaminated soil with CETSA and MA/AA. J Hazard Mater 366:177–183. https://doi.org/10.1016/j.jhazmat.2018.11.109
Xu L, Dai H, Skuza L, Wei S (2021) Comprehensive exploration of heavy metal contamination and risk assessment at two common smelter sites. Chemosphere 285:131350. https://doi.org/10.1016/j.chemosphere.2021.131350
Yang GL, Zheng MM, Tan AJ, Liu YT, Feng D, Lv SM (2021) Research on the mechanisms of plant enrichment and detoxification of cadmium. Biology. https://doi.org/10.3390/biology10060544
Yao H, Shi W, Wang X, Li J, Chen M, Li J, Chen D, Zhou L, Deng Z (2023) The root–associated Fusarium isolated based on fungal community analysis improves phytoremediation efficiency of *Ricinus communis* L. in multi metal-contaminated soils. Chemosphere 324:138377. https://doi.org/10.1016/j.chemosphere.2023.138377
Zhang X, Yang L, Li Y, Li H, Wang W, Ye B (2012) Impacts of lead/zinc mining and smelting on the environment and human health in China. Environ Monit Assess 184(4):2261–2273. https://doi.org/10.1007/s10661-011-2115-6
Zhang H, Guo Q, Yang J, Ma J, Chen G, Chen T, Zhu G, Wang J, Zhang G, Wang X, Shao C (2016) Comparison of chelates for enhancing *Ricinus communis* L. phytoremediation of Cd and Pb contaminated soil. Ecotoxicol Environ Saf 133:57–62. https://doi.org/10.1016/j.ecoenv.2016.05.036
Zhang J, Shao J, Jin Q, Li Z, Zhang X, Chen Y, Zhang S, Chen H (2019) Sludge–based biochar activation to enhance Pb (II) adsorption. Fuel 252:101–108
Zhang HH, Li C, Xu ZS, Wang Y, Teng ZY, An MJ, Zhang YH, Zhu WX, Xu N, Sun GY (2020a) Toxic effects of heavy metals Pb and Cd on mulberry (*Morus alba* L.) seedling leaves: photosynthetic function and reactive oxygen species (ROS) metabolism responses. Ecotoxicol Environ Saf 195:110469. https://doi.org/10.1016/j.ecoenv.2020.110469
Zhang J, Shao J, Jin Q, Zhang X, Yang H, Chen Y, Zhang S, Chen H (2020b) Effect of deashing on activation process and lead adsorption capacities of sludge-based biochar. Sci Total Environ 716:137016
Zhang X, Yu J, Huang Z, Li H, Liu X, Huang J, Zhuo R, Wu Z, Qin X, Gao Y, Wang M, Zhu Y (2021) Enhanced Cd phytostabilization and rhizosphere bacterial diversity of *Robinia pseudoacacia* L. by endophyte *Enterobacter* sp. YG–14 combined with sludge biochar. Sci Total Environ 787:147660. https://doi.org/10.1016/j.scitotenv.2021.147660
Zou T, Li T, Zhang X, Yu H, Huang H (2011) Lead accumulation and phytostabilization potential of dominant plant species growing in a lead–zinc mine tailing. Environ Earth Sci 65(3):621–630. https://doi.org/10.1007/s12665-011-1109-6